The Eurasia Proceedings of Science, Technology, Engineering & Mathematics (EPSTEM)
ISSN: 2602-3199

The Eurasia Proceedings of Science, Technology, Engineering and Mathematics (EPSTEM), 2025

Volume 38, Pages 567-574

IConTES 2025: International Conference on Technology, Engineering and Science

Effect of Cryogenic Treatment on the Microstructure of AlSi10Mg Alloy Produced by Selective Laser Melting

Pelin Sezer
Eskisehir Osmangazi University

Gamze Ertas
Eskisehir Osmangazi University

Hakan Gasan
Eskisehir Osmangazi University

Abstract: Research on the production of AlSi10Mg alloys using Selective Laser Melting (SLM), one of the additive manufacturing methods, is still ongoing. Since the use of SLM-fabricated parts in the as-built condition is not yet feasible, studies have particularly focused on post-processing. Moreover, the heat treatment parameters established for AlSi10Mg alloys produced by conventional methods do not necessarily show the same effects when applied to AM parts. Cryogenic treatment, which has been shown to have favorable effects for AlSi10Mg parts in the literature, and it increased the mechanical properties. In this study, AlSi10Mg block production was carried out via SLM using the predetermined process parameters and samples extracted from it. Then those samples were subjected to T6 heat treatment followed by cryogenic treatment for 12, 24, 36, and 48 hours. Subsequently, the samples were analyzed using optical microscopes to determine their microstructure and composition. Microstructural examinations showed that the effect of T6 heat treatment is the Si particle occurrence in Al matrix, after cryogenic treatment these particles changed relatively as the duration of cryogenic treatment changed.

Keywords: Selective laser melting, Cryogenic treatment, AlSi10Mg

Introduction

Within aluminum alloys, AlSi10Mg is known for its outstanding flowability and resistance to crack formation during solidification, which is due to its superior castability, weldability, low shrinkage, and low melting point. These qualities, together with high specific strength, excellent thermal and electrical conductivity, and extraordinary resistance to oxidation and corrosion, make AlSi10Mg a preferred material in the aerospace, automotive, defense, and general manufacturing industries. Silicon concentration promotes fluidity during manufacture, while magnesium strengthens the alloy and improves heat resistance (Vishnu et al., 2025). For Al alloys, the most common alloying elements are copper, magnesium, manganese, silicon, and zinc. Since the debut of metallic aircraft, alloys mostly made of aluminum have played a significant role in aerospace manufacturing. AlSi10Mg alloys are lighter than other aluminum alloys and less combustible than alloys with a high magnesium content (Desai et al., 2016).

An innovative heat treatment technique that is thought to be an alternative to conventional heat treatment is cryogenic treatment. Without altering the alloy's size or shape, it significantly impacts its microstructure and mechanical characteristics (Liu et al., 2025). Si element can gradually precipitate from the Al matrix during cryogenic treatment because the solubility of Si in Al alloys has a decreasing trend from high to low temperatures. It can reduce the coarse secondary particles along with boosting the precipitation of secondary

phases. It was found in a study that the average size of coarse particles in the sample exposed to a cryogenic temperature of -180˚C is just 6.9 µm smaller than that obtained in the circumstance of high temperatures. The formation of secondary phases that enhance the dispersion or cause precipitation and more homogenous distribution. One important strengthening method for high strength is precipitation strengthening especially (Yao et al., 2023).

An additive manufacturing technique called Selective Laser Melting (SLM), creates parts with complex internal structures. This method, which is based on CAD data, melts powder dispersed over a powder bed using an energy source along an identified scanning route to create a dense part. The superior microstructure produced by this method is responsible for the produced components' fine microstructure, which is a result of the SLM process's rapid cooling rate (Siyambaş & Turgut Y., 2022). A continuous eutectic structure of Al and Si is usually produced together with formed primary α-Al in the traditional AlSi10Mg casting method, where the solid solution of Si in aluminum breaks down easily during slow cooling and Si precipitates in the form of relatively coarse particles. Instead, the SLM technique produces a distinct microstructure in the AlSi10Mg components by continuously melting the material at a very high rate and then cooling it down rapidly. It is indicated distinct microstructures can observe a network of the eutectic Si phase along the boundary surrounding the α-Al phase and a cellular-dendritic structure of α-Al (Trevisian et al., 2017 & Semetse et al., 2025).

It is indicated that SLM produced AlSi10Mg has higher hardness than the cast parts, usually between 110 and 130 HV. The fast solidification rate during the SLM process, resulting in a small cellular microstructure with finely distributed hard silicon particles, is directly responsible for this increased hardness also after cryogenic treatment for 12h, and 24h the hardness increased 18.4% and 21.47% respectively (Gadlegaonkar et al., 2025 & Desai et al., 2016). It is indicated that CT results in the irregular volume shrinkage of the Al matrix and eutectic-Si networks and produces plastic deformation during the soaking period therefore, the samples retain compressive residual stress when they are reheated to room temperature. It is evident that the as-built and CT samples' XRD patterns are almost similar. Si precipitating out of the Al matrix after heat treatment (HT) and they observed the Si peaks in the HT samples are more intense than those in the other two samples the solid solubility of Si in the Al matrix is weakened by the HT. The extra Si caused the supersaturated α-Al to become thermodynamically unstable, which resulted in the removal of excess Si atoms from the α-Al matrix and the formation of individual Si particles during the HT. It is observed grain growth causes the intercellular network of eutectic-Si to change into polygonal Si particles that are evenly dispersed throughout the Al matrix (Zhou et al., 2022). CT promotes solute atom precipitation in the SLM AlSi10Mg alloy. Nevertheless, it has no appreciable effect on the eutectic Si networks or the morphologies and stacking structure of the melt pools and, the creation of atomic clusters is correlated with a progressive increase in the number of precipitated phases as duration of CT increases (Tang et al., 2025). According to these literature reviews, in this study the microstructural effect of SLM produced and cryogenic treated AlSi10Mg examined. Firstly, all samples exposed to T6 heat treatment and after that cryogenic treatment was held at -196˚C for 12, 24, 36 and 48h. Effects of the treatment time and its reasons are discussed.

Method

AlSi10Mg powder composition that is used for SLM production given in Table 1. The powder particle size distribution 20-63 µm and spherical shape. It consists of ~90% of aluminum and ~10% silicon. SLM production was carried out via Nikon SLM device. From this powder one block production was carried out SLM production parameters given in Table 2. Samples were taken from this block for investigation. The samples extracted from the block were subjected to the metallographic sample preparation steps in order: mounting, grinding, and polishing. For microstructural characterization Nikon Eclipse L150 optical microscope was used. Samples were etched with the Keller's reagent (95 mL distilled water, 2.5 mL HNO3, 1 mL HF, and 1.5 mL HCl). In an atmospheric heat treatment furnace, test materials were solution treated for 30 min. at 530˚C, water quenched to room temperature, then aged for six hours at 165˚C, and then cooled in atmospheric conditions (T6). Following that, four samples were cryogenic treated for 12, 24, 36, and 48 hours at -196˚C using liquid nitrogen. Hardness test was carried out via Future-Tech FM800 microhardness tester 100 gf and 10 sec. Tests were done with 5 indents in distance 25µm.

Table 1. The AlSi10Mg powder chemical composition (Nikon SLM Solutions, 2024)

Element	Al	Si	Fe	Cu	Mn	Mg	Zn	Ti	Ni	Pb	Sn	Total each	Total others
% wt	Balance	9-11.0	0.55	0.05	0.45	0.25	0.10	0.15	0.05	0.05	0.05	0.05	0.15

Table 2. SLM production parameters.

Parameters	
Laser power	300 W
Scanning speed	700 mm/s
Scanning strategy	Stripe
Beam diameter	0.1 mm
Hatch distance	0.17 mm

Results and Discussion

Microstructural Examination

Microstructural examinations were carried out using an optical microscope (OM). Figure 1 presents the microstructure images of the as-built (AB) sample at a) 50× magnification and b) 200× magnification. As seen in Figure 1.a, layer-by-layer melting traces, also known as melt pool boundaries, are visible due to the additive manufacturing process. This is attributed to the rapid solidification rates in the samples produced by additive manufacturing (Koç et al., 2025). In Figure 1.b, very fine eutectic silicon microstructures can be observed. The melt pools were formed as continuous and wide. It was observed to have a regular geometry with a segmental circular shape and these formations exhibiting a “fish-scale” morphology.

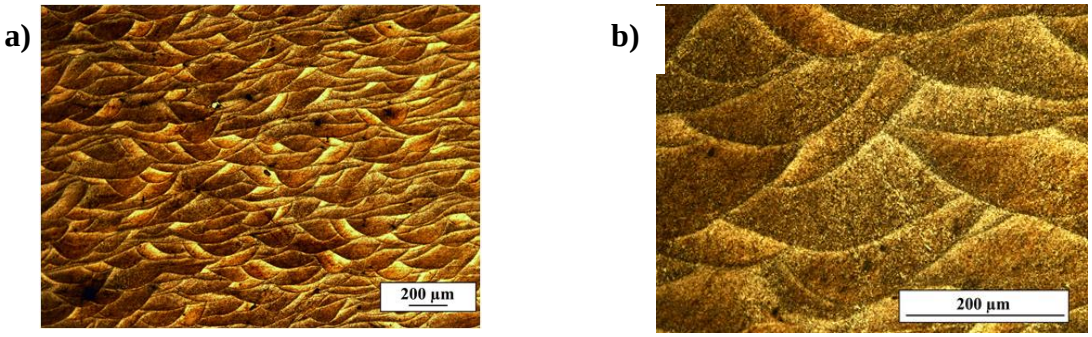

Figure 1. Microstructural images belong to as-built (AB) sample a) 50x magnification b) 200x magnification.

Figure 2 presents the microstructure images of the sample subjected to T6 heat treated, 12, 24, 36 and 48h cryogenically treated samples. As seen in Figure 2.a, c, g and i, the melt pool traces observed in the as-built sample have disappeared, with the effect of T6 heat treatment conditions. Additionally, the interlayer pores stand out. The Si networks formed on the Al matrix are observed to be finer (Figure 2a, c, g and i) compared to those in the as-built sample (Figure 1.a). In Figure 2b, d, f, h and j, this distribution can be seen more clear and more homogenous. From microstructural images, it is observed that the T6 heat treatment helped to reduce the melt pool appearance and a more homogeneous microstructure distribution was obtained. However, in sample 24h cryogenic treated, these traces are still slightly noticeable (Figure 2.e-f). The expectation here is that removal will be observed in all melt pools, but this effect may have re-formed after the cryogenic treatment. All images exhibit the typical microstructural characteristics of the AlSi10Mg alloy after T6 heat treatment. Following the solution treatment and artificial aging steps, a cellular Al matrix with finely distributed Si particles is observed. The distinct melt pool boundaries seen in the as-built condition have largely disappeared after the T6 process, resulting in a more homogeneous and uniform phase distribution.

Figure 3 includes the examination of the top view of the samples AB, after T6 heat treatment, and CT for 12, 24, 36, and 48 hours. Figures 3a–b, correspond to the AB sample. Although the microstructure appears visually different from the side section, it can be stated that this structure is also formed by the Si network generated by the laser input. Similar overlapped laser tracks can be seen in the top view of the specimen, but in the side view, the shape of the molten pool shifts from shallow to deep (Figure 1.a-b). Furthermore, the pores at the bottom of sample, referred to as keyhole flaws, attest to the fact that the keyhole effect caused material vaporization. These traces seem brighter in the OM image because their boundaries etch more strongly. The presence of fibrous separated eutectic Si particles in these particular areas is what causes the increased susceptibility to chemical etching. There are also irregular porosities in the sample which is the primary source is the balling phenomena brought on by the degrading metallurgical bonding (Dong et al., 2020).

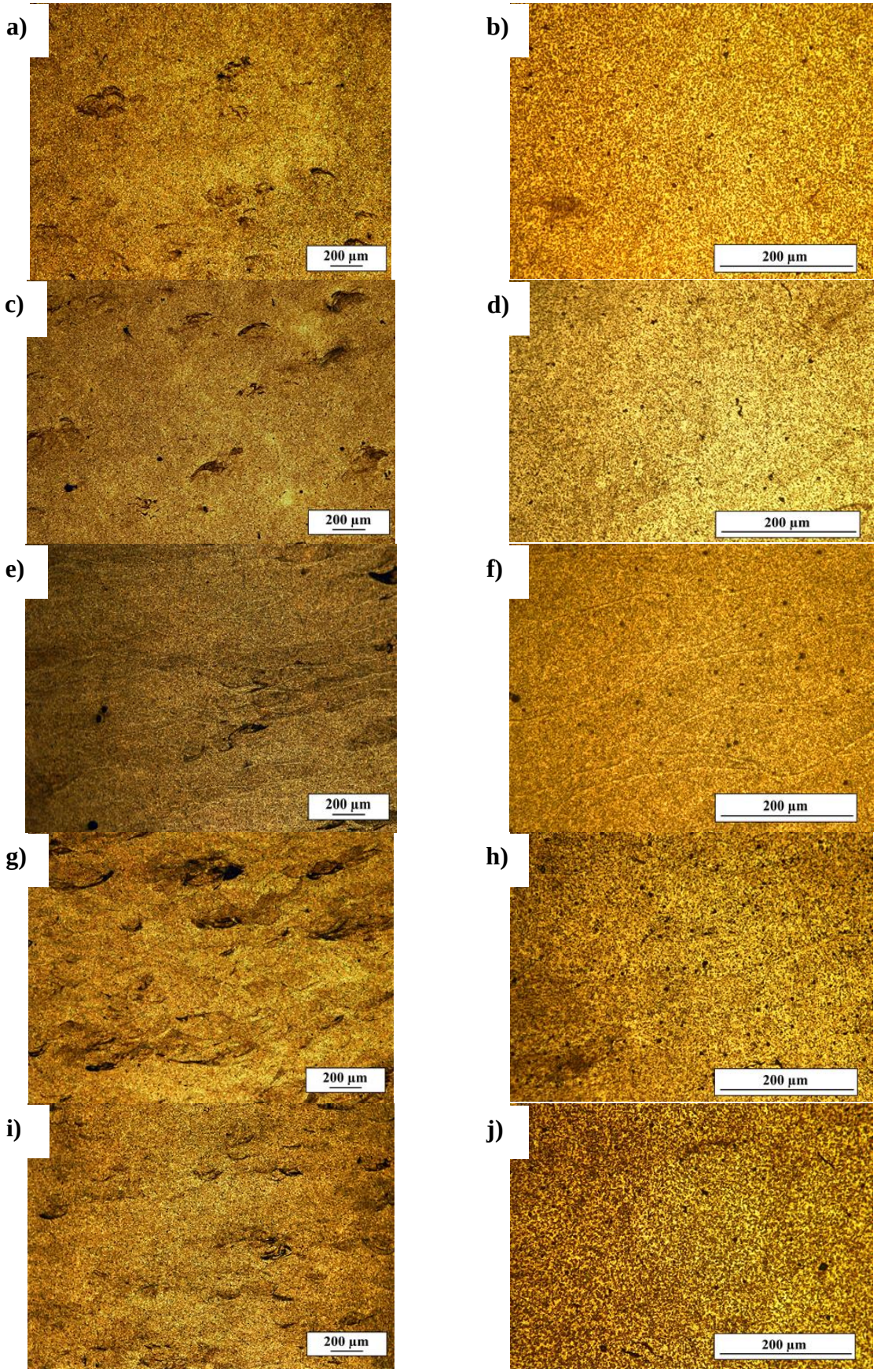

Figure 2. Microstructural images belong to side section of a-b) T6 heat treated, c-d) T6+12h cryogenic treated, e-f) T6+24h cryogenic treated, g-h) T6+36h cryogenic treated, i-j) T6+48h cryogenic treated 50x and 200x magnifications respectively.

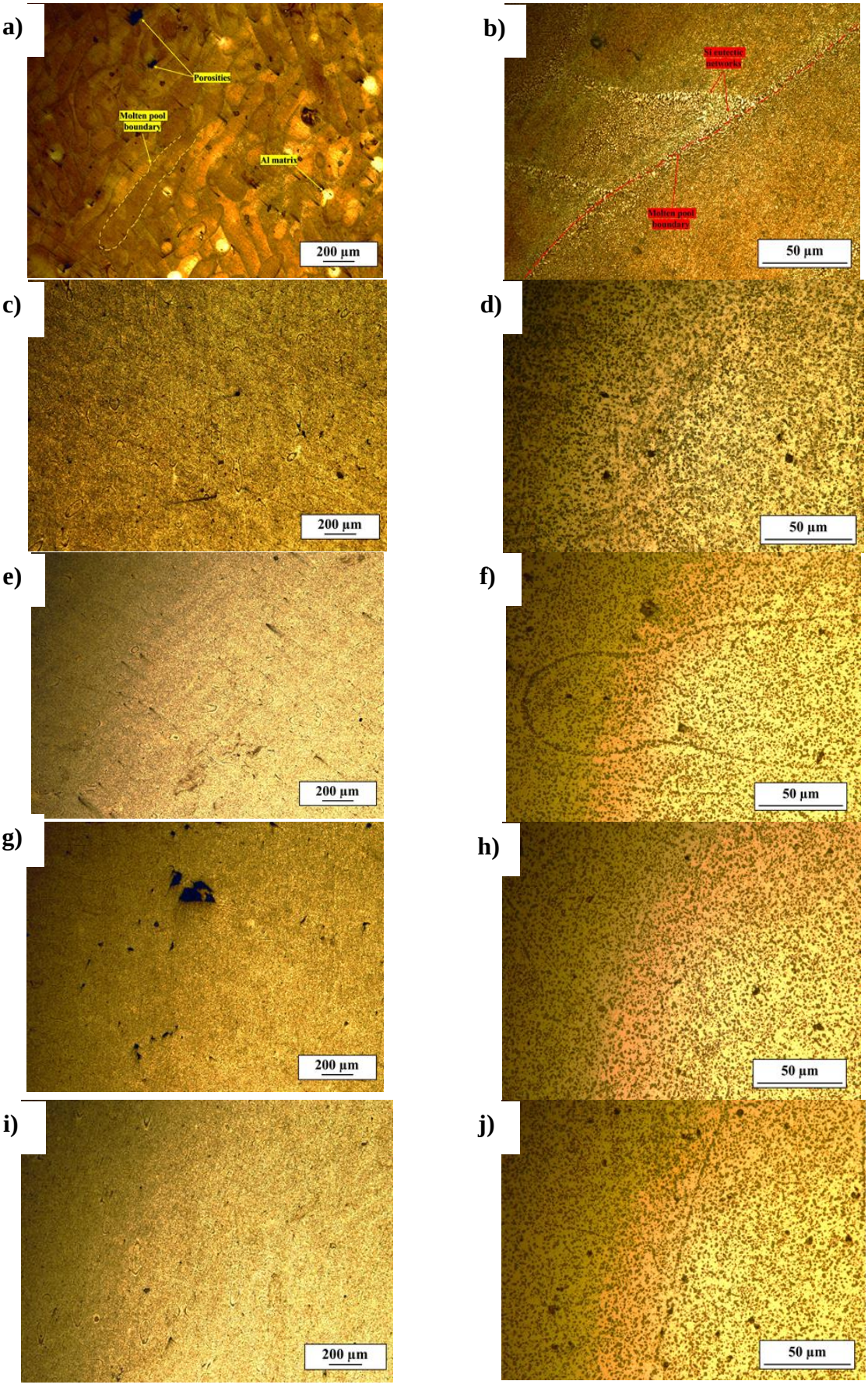
a)
Porosities
Molten pool boundary
Al matrix
200 µm
b)
Si eutectic networks
Molten pool boundary
50 µm
c)
200 µm
d)
50 µm
e)
200 µm
f)
50 µm
g)
200 µm
h)
50 µm
i)
200 µm
j)
50 µm

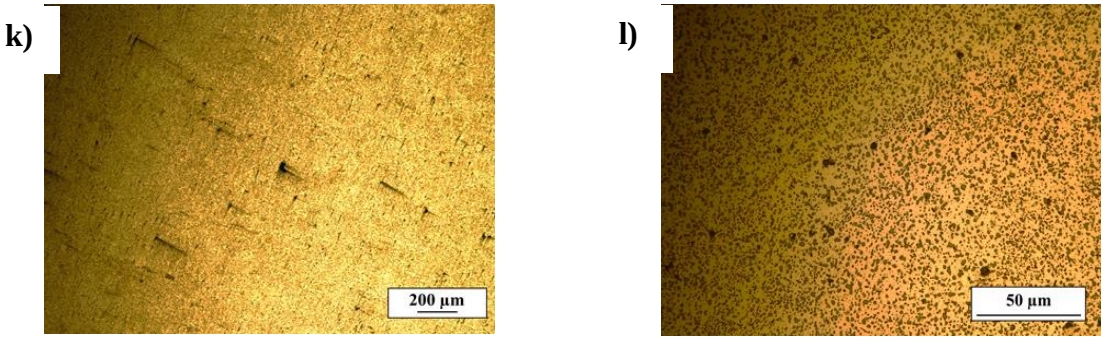

Figure 3. Microstructural images belong to top section of a-b) as-built, c-d) T6 heat treated, e-f) T6+12h cryogenic treated, g-h) T6+24h cryogenic treated, i-j) T6+36h cryogenic treated, k-l) T6+48h cryogenic treated 50x and 500x magnifications respectively.

After the T6 heat treatment (Figure 3.c–d), similar to the side view observations, the microstructure became homogeneous, and the scanning tracks and molten pool patterns disappeared. However, the Si eutectic structure transformed into Si precipitate particles. Although these precipitates eliminated most of the molten pool features, traces of such patterns can still be slightly observed in the structure, replaced by Si precipitates. After 12 hours of cryogenic treatment, a structure similar to that of the T6 heat-treated sample was observed (Figure 3.e). However, compared to the T6 heat treatment, it is possible to mention relatively smaller Si particles, it was observed that the Si particles were grouped together within the structure, making the Al phase more distinguishable (Figure 3.f). When Figure 3.g is examined, a large number of pores can be noticed. Beneath these pores, a structure similar to that of the T6 heat-treated sample is observed. Upon closer examination of the precipitates, it can be seen that the localized particles present after the 12-hour cryogenic treatment have been replaced by a more homogeneous appearance (Figure 3.h). The 48-hour cryogenic treatment made the microstructure more homogeneous, and the precipitates were uniformly distributed in various sizes, both large and small (Figure 3 k-l).

Hardness Results

Figure 4 shows that hardness results belong to as-built, T6 heat treated, 12, 24, 36 and 48h CT samples. In as-built condition hardness measured as 107.42 HV which is higher than the cast conditions. This can be result of the rapid cooling. After T6 heat treatment this result increased to 120.8 HV. This result is attributed to the elimination of the melt pool structure present in the microstructure under additive manufacturing conditions, the precipitation of Si particles, and the formation of a more homogeneous microstructure. After 12h cryogenic treatment hardness decreased to 111.8HV. Increasing the cryogenic treatment time increased the hardness to 117.4 HV. And then 36 and 48 hours decreased hardness to 112.16 and 115.8 HV respectively.

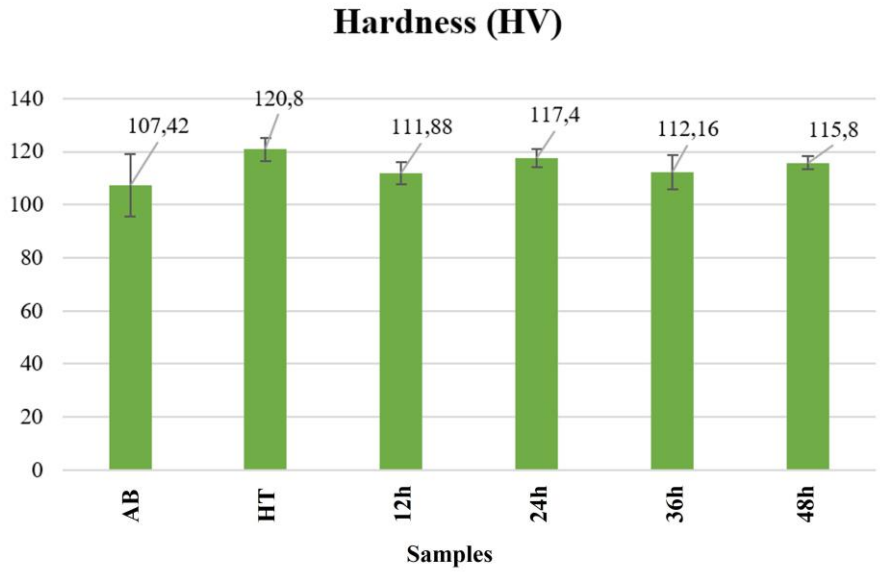

Figure 5. Hardness results belong to samples.

As reported in the literature, Si particle precipitations exhibit variability that can influence the mechanical properties of AlSi10Mg alloys. Accordingly, the slight changes observed in hardness can be attributed to the increase or decrease of these precipitates. In the AB condition, the sample has completely different microstructure, whereas after T6 heat treatment, distinct Si particles are shown. The hardness value, which reached around 120 HV, can be associated with the presence of these particles. Owing to cryogenic treatment, variations in the size and distribution of precipitates initially caused a reduction in hardness, followed by an increase at 24 hours of treatment, and then a subsequent decreasing trend nearly similar 36h and 48h CT samples.

Conclusion

In this study, the microstructural changes, hardness values of AlSi10Mg samples produced by the SLM method were investigated after T6 heat treatment and subjected to cryogenic treatment at –196 °C for holding times of 12, 24, 36, and 48 hours. The results are as follows:

- The AB images show differences between the side and top views; however, the same fundamental structural formations have been observed in both-Si eutectic phase.
- After the T6 heat treatment, the deposition traces and fish-scale melt pool patterns observed in the as-built (AB) samples disappeared, giving way to the formation of Si precipitates both side and top views of the sample.
- While more homogeneous Si precipitates were present in the 12-hour and 48-hour cryogenic treatments, the same level of homogeneity could not be achieved in the microstructures of the 24-hour and 36-hour treatments – however, no significant difference has been observed.
- The highest hardness was obtained after the T6 heat treatment because of the Si particles, while the change in hardness with cryogenic treatment was not of significant magnitude.

Recommendations

In addition to the analyses performed on the AlSi10Mg samples, SEM-TEM analysis could be preferred for the investigation of smaller precipitates. Furthermore, alternative analytical methods can be employed for monitoring particle size. Wear analyses could be held results further contribute to literature.

Scientific Ethics Declaration

* The authors declare that the scientific ethical and legal responsibility of this article published in EPSTEM journal belongs to the authors.

Conflict of Interest

* The authors declare that they have no conflicts of interest

Funding

* This study is supported within the scope of the TÜBİTAK 2209-B program (Project No: 1139B412408088).

Acknowledgements or Notes

* This article was presented as an oral presentation at the International Conference on Technology, Engineering and Science (www.icontes.net) held in Antalya/Türkiye on November 12-15, 2025.

References

Desai, R. S., Joshi, A. G., & Kumar, S. (2016). Study on influence of cryogenic treatment on mechanical properties of AlSi10Mg alloy. *International Journal of Research in Engineering and Technology, 5*, 53.

Dong, S., Zhang, X., Ma, F., Jiang, J., & Yang, W. (2020). Research on deposited tracks and microstructures of AlSi10Mg alloy produced by selective laser melting. *Applied Physics A, 126*(8), 643.

Gadlegaonkar, N., Bansod, P. J., Lakshmikanthan, A., & Bhole, K. (2025). A review on additively manufactured AlSi10Mg alloy: Mechanical, tribological, and microstructure properties. *Journal of Mines, Metals & Fuels*, *73*(1).

Koç, E., et al. (2025). Effects of retrogression and re-aging heat treatments on microstructure, phase transformations, hardness, and dry sliding wear in powder bed laser fusion/AlSi10Mg. *Journal of Materials Engineering and Performance*, 1-12.

Liu, Y., Chen, Z., Huang, Y., Jing, L., & Niu, X. (2025). Effect of cryogenic treatment on 7A09 aluminum alloy and optimization of process parameters. *Journal of Materials Engineering and Performance*, *34*(17), 19752-19766.

Nikon SLM Solutions. (2024). *Material data sheet: AlSi10Mg DIN EN 1706 / EN AC-43000*. Retrieved from https://nikon-slm-solutions.com/wp-content/uploads/2025/02/mds5123.pdf

Semetse, L., Olaogun, O., & Olubambi, P. (2025). Sliding wear behaviour of heat treated selective laser melted AlSi10Mg alloy. *SSRN*.

Siyambas, Y., & Turgut, Y. (2022). Seçici lazer ergitme (SLM) yöntemi ile üretilen AlSi10Mg alaşımlı parçalarda kusurlar, mekanik özellikler ve yüzey pürüzlülüğü-Bir araştırma. *Gazi Üniversitesi Fen Bilimleri Dergisi Part C: Tasarım ve Teknoloji, 10*(2), 368-390.

Tang, P., Wang, H., Cheng, X., Zang, J., & Zhao, Y. (2025). Effects of cryogenic thermal cycling treatment on microstructure, mechanical properties and residual stress of selective laser melted AlSi10Mg alloy. *Materials Science and Engineering: A, 944*, 148963.

Tonolini, P., Montesano, L., Tocci, M., Pola, A., & Gelfi, M. (2021). Wear behavior of AlSi10Mg alloy produced by laser-based powder bed fusion and gravity casting. *Advanced Engineering Materials, 23*(10), 2100147.

Trevisan, F., Calignano, F., Lorusso, M., Pakkanen, J., Aversa, A., Ambrosio, E. P., ... & Manfredi, D. (2017). On the selective laser melting (SLM) of the AlSi10Mg alloy: Process, microstructure, and mechanical properties. *Materials, 10*(1), 76.

Vishnu, V., Prabhu, T. R., & Vineesh, K. P. (2025). Effect of hard anodizing and T6 heat treatment on the dry sliding wear behavior of AlSi10Mg fabricated by direct metal laser sintering. *Wear, 564*, 205677.

Yao, E., Zhang, H., Ma, K., Ai, C., Gao, Q., & Lin, X. (2023). Effect of deep cryogenic treatment on microstructures and performances of aluminum alloys: A review. *Journal of Materials Research and Technology, 26*, 3661-3675.

Zhou, C. A., Sun, Q., Qian, D., Liu, J., Sun, J., & Sun, Z. (2022). Effect of deep cryogenic treatment on mechanical properties and residual stress of AlSi10Mg alloy fabricated by laser powder bed fusion. *Journal of Materials Processing Technology, 303*, 117543.

Author(s) Information

Pelin Sezer
Eskisehir Osmangazi University,
Faculty of Engineering and Architecture,
Department of Metallurgical and Materials Engineering
Meşelik Kampüsü Odunpazarı/Eskişehir, Türkiye
Contact e-mail: *pelin.sezer@ogu.edu.tr*

Gamze Ertas
Eskisehir Osmangazi University,
Faculty of Engineering and Architecture,
Department of Metallurgical and Materials Engineering
Meşelik Kampüsü Odunpazarı/Eskişehir, Türkiye

Hakan Gasan
Eskisehir Osmangazi University,
Faculty of Engineering and Architecture,
Department of Metallurgical and Materials Engineering
Meşelik Kampüsü Odunpazarı/Eskişehir, Türkiye

To cite this article:

Sezer, P., Ertas, G., & Gasan, H. (2025). Effect of cryogenic treatment on the microstructure of AlSi10Mg alloy produced by selective laser melting. *The Eurasia Proceedings of Science, Technology, Engineering and Mathematics (EPSTEM), 38*, 567-574.